

Article

## Structure-based Rational Design of Novel Inhibitors against Fructose-1,6-Bisphosphate Aldolase from *Candida albicans*

Xinya Han, Xiuyun Zhu, Zongqin Hong, Lin Wei, Yanliang Ren, Fen Wan, Shuaihua Zhu, Hao Peng, Li guo, Li Rao, Lingling Feng, and Jian Wan

*J. Chem. Inf. Model.*, **Just Accepted Manuscript** • Publication Date (Web): 05 May 2017

Downloaded from <http://pubs.acs.org> on May 5, 2017

### Just Accepted

"Just Accepted" manuscripts have been peer-reviewed and accepted for publication. They are posted online prior to technical editing, formatting for publication and author proofing. The American Chemical Society provides "Just Accepted" as a free service to the research community to expedite the dissemination of scientific material as soon as possible after acceptance. "Just Accepted" manuscripts appear in full in PDF format accompanied by an HTML abstract. "Just Accepted" manuscripts have been fully peer reviewed, but should not be considered the official version of record. They are accessible to all readers and citable by the Digital Object Identifier (DOI®). "Just Accepted" is an optional service offered to authors. Therefore, the "Just Accepted" Web site may not include all articles that will be published in the journal. After a manuscript is technically edited and formatted, it will be removed from the "Just Accepted" Web site and published as an ASAP article. Note that technical editing may introduce minor changes to the manuscript text and/or graphics which could affect content, and all legal disclaimers and ethical guidelines that apply to the journal pertain. ACS cannot be held responsible for errors or consequences arising from the use of information contained in these "Just Accepted" manuscripts.



ACS Publications

# Structure-based Rational Design of Novel Inhibitors against Fructose-1,6-Bisphosphate Aldolase from *Candida albicans*

Xinya Han,<sup>‡,a</sup> Xiuyun Zhu,<sup>‡,a</sup> Zongqin Hong,<sup>‡,a</sup> Lin Wei,<sup>a</sup> Yanliang Ren,<sup>a,\*</sup> Fen Wan,<sup>a</sup> Shuaihua  
Zhu,<sup>a</sup> Hao Peng,<sup>a</sup> Li Guo,<sup>b</sup> Li Rao,<sup>a</sup> Lingling Feng,<sup>a</sup> Jian Wan,<sup>a,\*</sup>

<sup>a</sup> Key Laboratory of Pesticide & Chemical Biology (CCNU), Ministry of Education, Department  
of Chemistry, Central China Normal University, Wuhan 430079, China

<sup>b</sup> Hubei Environmental Monitoring Central Station, Wuhan 430072, Hubei, China

**KEYWORDS** Class II fructose-1,6-bisphosphate aldolases (FBA-II), Ca-FBA-II inhibitors, *C.*  
*albicans*, rational drug design, novel antifungal pathogens

**ABSTRACT** Class II fructose-1,6-bisphosphate aldolases (FBA-II) are attractive new targets for the discovery of drugs to combat invasive fungal infection, because they are absent in animals and higher plants. Although several FBA-II inhibitors have been reported, none of these inhibitors exhibit antifungal effect so far. In this study, several novel inhibitors of FBA-II from *C. albicans* (Ca-FBA-II) with potent antifungal effects were rationally designed by jointly using a specific protocols of molecular docking-based virtual screening, accurate binding-conformation evaluation strategy, synthesis and enzymatic assays. The enzymatic assays reveal that the compounds **3c**, **3e–g**, **3j** and **3k** exhibit high inhibitory activity against Ca-FBA-II ( $IC_{50} < 10 \mu M$ ), and the most potential inhibitor is **3g**, with  $IC_{50}$  value of  $2.7 \mu M$ . Importantly, the compounds **3f**, **3g** and **3l** possess not only high inhibitions against Ca-FBA-II, but also moderate antifungal activities against *C. glabrata* ( $MIC_{80} = 4\text{--}64 \mu g/mL$ ). The compounds **3g**, **3l** and **3k** in combination with fluconazole ( $8 \mu g/mL$ ) displayed significantly synergistic antifungal activities ( $MIC_{80} < 0.0625 \mu g/mL$ ) against resistant *Candida* strains, which are resistant to azoles drugs. The probable binding modes between **3g** and the active site of Ca-FBA-II have been proposed by using the DOX (Docking, ONIOM and XO) strategy. To our knowledge, no FBA-II inhibitors with antifungal activities against wild type and resistant strains from *Candida* were reported previously. The positive results suggest that the strategy adopted in this study are a promising method for the discovery of novel drugs against azole-resistant fungal pathogens in the future.

## INTRODUCTION

Fungal infections are a serious public health problem.<sup>1</sup> *Candida* is the primary systemic fungus affecting humans. This fungus is usually existed in the oral and gastrointestinal tracts in many individuals as a commensal pathogen but can also cause severely oral and vaginal infections when normal fungus-host were disturbed. For severely immunocompromised patients, *Candida* can led to the life-threatening systemic infections.<sup>2-4</sup>

Limited antifungal drugs can be used against *Candida* infections. The drugs<sup>5-8</sup> in routine clinical use included, echinocandins, polyenes, azoles and flucytosine (5-FC). Polyenes (E. g. amphotericin B) are regard as bind ergosterol of the fungal plasma membrane; The azoles targeted CYP51 (sterol 14 alpha-demethylase) can inhibited ergosterol biosynthesis; The echinocandins mainly inhibit glucansynthesis.<sup>8</sup> 5-FC was first synthesized in 1957. Monotherapy with 5-FC is limited as for the frequent development of resistance. However, 5-FC can be used in combination with amphotericin B to treat severe systemic mycoses.<sup>5, 9-11</sup> Azoles are the most well-known antifungal drugs worldwide. However, due to the extensive use of these drugs in humans, the resistances of pathogenic microorganisms to current drug are a significant threat to public health.<sup>12, 13</sup> Azole derivatives targeting CYP51 are heme iron coordinating compounds with the potential to also interact with human CYPs; via nonspecific drug-metal binding, which can lead to various azole drug side effects.<sup>14</sup> Therefore, there is an urgent need to quickly discover new selective targets.

Fructose-1,6-bisphosphate aldolase (FBA, EC4.1.2.13) catalyzes the reversible aldol condensation of dihydroxyacetonephosphate (DHAP) and glyceraldehyde 3-phosphate (GAP) to yield fructose-1,6-bisphosphate (FBP),<sup>15-17</sup> and can be characterized two distinct classes as reported by Therisod (Figure 1).<sup>1</sup> Class I FBA (FBA-I), which is existed in higher organisms and

some prokaryotes, forms a Schiff-base intermediate between a lysine residue of the active site and the keto substrate. In contrast, class II FBA (FBA-II) used the divalent metal ion to polarize the keto carbonyl group on the substrate, and to stabilize the enediolate intermediate. Since FBA-II is existed in pathogenic microbes (E. g. fungus, bacteria and parasites) and absented in animals, this enzyme is considered a particularly attractive new target.<sup>16, 18-20</sup> The importance of FBA-II has been illustrated by knockout studies, including *M. tuberculosis*,<sup>19</sup> *S. galbus*,<sup>20</sup> *B. subtilis*,<sup>21</sup> *P. aeruginosa*<sup>22, 23</sup> and *S. pneumonia*.<sup>24</sup> Additionally, Brown et al.<sup>25</sup> have examined the effects of depleting this enzyme in *C. albicans* to check the validity of FBA-II as the target of the antifungal drug. Their results showed that when FBA-II is depleted to below 5% of the wild-type levels, the growth of *C. albicans* will be blocked. Therefore, the necessity of FBA-II and the absence of human homologue have made FBA-II most potent as a drug target. Additionally, the sequence conservation between fungal aldolases is significantly high (>80%), which suggests that developing broad-spectrum antifungal drug that can selectively inhibit aldolase in fungus might be possible.

To our knowledge, several analogues<sup>1, 16, 26, 27</sup> of FBP, DHAP and phospho-glycolohydroxamic acid (PGH) have been reported to have high inhibitory activities against FBA-II, and some of these inhibitors also highly inhibit the FBA-II from *C. albicans* (Ca-FBA-II). However, no inhibition against the growth of cultivated pathogens has been observed by using these compounds. It may be that the phosphate groups of these compounds are very polar, and they are thus hard to cross biological membranes by simple diffusion. Therefore, the idea of preparing inhibitors of FBA-II as potential new drug has received limited attention. Herein, we report positive progress in this field. With a structure-based drug design strategy, a series of novel Ca-FBA-II inhibitors with potent antifungal effects against wild type and resistant strains from

*Candida* have been successfully designed and synthesized in the present study. The probable binding-modes between the representative hit compounds and Ca-FBA-II were analyzed by jointly using the DOX (Docking, ONIOM and XO) strategy,<sup>28</sup> molecular dynamics (MD) simulations and enzymatic assays.

## RESULT AND DISCUSSION

**Building the 3D conformation of Ca-FBA-II.** Recent reviews<sup>29</sup> have suggested that a sequence identity that are higher than 30% is indicative of similar 3D structures. Our ClustalW2<sup>30</sup> analysis showed that the FBA-II from *E. coli* (Ec-FBA-II)<sup>31</sup> shared the highest identity (56.3%, as shown in Figure S1) with Ca-FBA-II (GenBank Number: 224471817), permitting a straightforward sequence alignment and guaranteeing the quality of the homology model. Therefore, using Ec-FBA-II (PDB ID: 1B57) as template, the plausible homology model of Ca-FBA-II was performed with the SWISSMODEL server.<sup>32</sup> To reduce steric clashes, a staged minimization was performed using SYBYL X1.3.<sup>33</sup> The quality of the homology model of Ca-FBA-II was assessed with PROCHECK,<sup>34</sup> ProQ,<sup>35</sup> ProSA-web,<sup>36, 37</sup> and QMEAN.<sup>38</sup> The assessments revealed that the LGscore in ProQ was 6.606 (scores  $\geq 2.5$  indicate a very good model), the QMEAN score was 0.533 (reliable model lies between 0 and 1), and the Z-score from ProSA-Web was  $-9.57$  (Figure S2). The quality of the 3D model structure of Ca-FBA-II were also confirmed by Ramachandran plot analyses of PROCHECK<sup>34</sup> (Figure S3), the results indicated that 88.5 % of the residues were distributed in the favored regions, 10.5 % were in the additionally allowed regions, 0.5 % in the generously allowed regions, while only 0.5 % of the residues were in the disallowed regions. These assessment results indicated that the backbones of the modeled 3D structure of Ca-FBA-II were reasonable.

**Identifying the binding modes of Ca-FBA-II and FBP.** Although Ec-FBA-II shares the highest identity (56.3%) with Ca-FBA-II, no corresponding substrate is complexed in Ec-FBA-II. However, the active site of Ca-FBA-II is also highly identical to that of the FBA-II from *Mycobacterium tuberculosis* (Mt-FBA-II). Furthermore, the X-ray crystallographic structure of Mt-FBA-II complexed with its substrate, an acyclic keto form of FBP, has been resolved (PDB: 3ELF).<sup>19</sup> To generate a rational active site region, the resultant model structure of Ca-FBA-II and the crystal structure of Mt-FBA-II were superimposed each other, and the substrate (FBP) was then merged into the corresponding pocket of Ca-FBA-II. All atoms located within 6.5 Å from any atom of FBP were selected as part of the active site of Ca-FBA-II, the corresponding residues were considered to be involved in the active site if one or more of their atoms were selected.

As reported in previous studies,<sup>19, 31, 39</sup> using a divalent metal ion, FBA-II could polarize the keto carbonyl group of the substrate and stabilize the enediolate intermediate formed during catalysis. Thus, coordination with a divalent metal ion is a predominant factor in ligands binding, which has indeed been confirmed by the crystallographic structure of FBA-II complexed with its ligands.<sup>16, 19</sup> Therefore, the Zn (II) ion is the most important pharmacophore for design of novel inhibitors.

**Docking-based virtual screening and identification of the probe molecule.** Using the active cavities of the 3D model structure of Ca-FBA-II generated above, a set of virtual screening strategies (illustrated in Figure S4) were employed to obtain inhibitors targeting Ca-FBA-II. For the first step, a 2D ligand-based search was performed to preselect the compounds from the Specs database based on Lipinski's rule of five,<sup>40</sup> which is usually used as a guideline to identify drug candidates that are more probably yield cell permeable compounds, and also allow oral

administration. After the 2D ligand-based search, about 110,000 compounds were screened for the subsequent docking-based virtual screening. All preselected 2D compounds were transformed into 3D conformations using the CONCORD module of SYBYL X1.3.<sup>33</sup> As discussed above, the Zn (II) metal ion in the active site is essential to the catalysis of Ca-FBA-II. Thus, the design of inhibitors centers on a synthetically accessible scaffold that positions a Zn (II) ion binding group. FlexX-Pharm enables pharmacophore-type constraints to guide ligand docking.<sup>41</sup> Thus, we define spatial and pharmacophore constraints in the docking screening process based on Ca-FBA-II out of Specs database as mentioned before. The spatial constraint defined by a distance from the Zn (II) ions of 3.0 Å or less was used in the Flex-Pharm docking. Under this constraint, only those compounds docked into the cavity of Ca-FBA-II that met this restrictive condition were immediately selected for further judgment using a scoring function. After the FlexX-Pharm procedures were applied to Ca-FBA-II, approximately 30,000 compounds were selected.

Surflex-Dock<sup>42</sup> usually dock ligands into the binding site of a protein by using an empirical scoring function and a patented search engine. This program was particularly successful in eliminating false positive results and retaining a large amounts of active compounds.<sup>42, 43</sup> Therefore, Surflex-Dock experiments were performed on Ca-FBA-II, and approximately 10,000 compounds were selected. Subsequently, those compounds with similar backbones were collected into one category. Finally, the hit compounds (~500) were selected out by jointly considering the docking score and docked conformations of the compounds. The virtual screening strategy adopted in this study was also documented in our previous studies.<sup>44-46</sup> Only compounds with a high docking score that interacted with Zn (II) ion in Ca-FBA-II were selected.



Finally, thirty representative potential compounds were purchased from Specs Corporation, and the corresponding inhibitory activities against Ca-FBA-II were examined (Table S1).

As observed in Table S1, compounds **1**, **FBA10** and **FBA26** exhibited high inhibitory ratios (> 70%) against Ca-FBA-II, therefore, the IC<sub>50</sub> values of these three compounds were determined. Compound **1** exhibited a lower IC<sub>50</sub> value (17 μM) against Ca-FBA-II than the other two compounds. Therefore, compound **1** was selected as a probe molecule for further development and optimization to obtain more potent inhibitors of Ca-FBA-II.

**Identifying the binding mode of Ca-FBA-II and compound 1.** To discover more potent inhibitors, accurate insight into the binding mode of the probe molecule **1** was essential. To obtain the starting-point binding-conformation of **1** and Ca-FBA-II, a DOX strategy, which has been documented previously,<sup>28</sup> was applied to predict the most reasonable binding-conformation of Ca-FBA-II and **1**. Firstly, compound **1** was docked into Ca-FBA-II using the Surflex-Dock module in Sybyl-X1.3 software to generate as much binding-conformation of **1** with Ca-FBA-II as possible. After the docking procedure, approximately 200 poses with different binding-conformations were obtained. Then, poses with similar conformations (RMSD < 0.35 Å) were aggregated into one category, and we selected one representative pose from each category for further binding-energy calculations using three-layer ONIOM (ONIOM3) method in Gaussian 09 software package.<sup>47</sup> In the ONIOM3 calculations, compound **1** was set as the high layer with a sphere model, which was calculated at the B3LYP/6-31G(d) theoretical level; the important residues within 10 Å depth from any given atom of **1** were considered to be the medium layer (M), which was calculated using a semi-empirical method (PM6). The low layer (L) consisted of the entire enzyme system, and was calculated by using the AMBER force field. To consider the flexibility of **1** and the active site of Ca-FBA-II, the top 10 poses with the lowest binding-

energies were selected for further geometric optimization using XO methods.<sup>48</sup> Finally, the binding-conformation with the lowest binding-energy as optimized with XO was selected, as illustrated in Figure 2A.

As seen from Figure 2A, the hydroxyl group of compound **1** appears to be very important for the binding of **1** to Ca-FBA-II. The hydroxyl group could coordinate with the Zn (II) ion. In fact, the hydroxyl group is easily ionized in solution when it is coordinated with the metal. Thus, the hydroxyl group on the benzene ring of **1** was set in the ionized state in the present investigation. The hydrogen atom on the hydroxyl group is likely to be transferred to the surrounding Asp109, and the oxygen atom of the phenolic hydroxyl group could also form two hydrogen bonds with the COOH moiety of Asp109 and the NH<sub>2</sub> moiety of Asn287. Additionally, one of the carbonyl groups of **1** appears to form a hydrogen bond with the NH moiety of Glu182, and the other carbonyl group is likely to form a hydrogen bond with Asn36. In the middle region of **1**, one hydrogen bond between Asp289 and the NH moiety of **1** could be observed. The nitro group of **1** is likely to form two hydrogen bonds with Ser268 and Thr290. To further consider the flexibility of the whole protein (Ca-FBA-II), we took the complex (Ca-FBA-II and **1**) optimized by the XO method<sup>48</sup> as the starting point conformation, and a molecular dynamics (MD) simulation was further performed using the Amber 12 program.<sup>47</sup> Plots of the RMSD and simulation time are illustrated in Figure 3. The black line represents the RMSD of the backbone Ca atoms of the complex (Ca-FBA-II and **1**) between simulated trajectories and initial structure, whereas the pink line represents the corresponding RMSD of compound **1**. In Figure 3, the black line nearly achieves a dynamic convergence at approximately 16 ns, whereas the pink line rapidly arrives at a dynamic convergence with an RMSD value of 1 Å. The conformation of the complex (Ca-FBA-II and **1**) with the lowest kinetic energy was obtained from the simulation trajectory (16-20

ns). The binding mode of Ca-FBA-II to **1** optimized according to the MD simulations in a protein environment is illustrated in Figure 2B. Compared with Figure 2A, Figure 2B illustrates that the O<sup>-</sup> moiety of **1** remains in coordination with the Zn (II) ion, this suggest that the O<sup>-</sup> moiety of **1** is essential to the binding of **1** to Ca-FBA-II. Although the binding mode optimized with XO shows no obvious coordination between the carbonyl group and the Zn (II) ion, the MD result reveals that one of the carbonyl groups of **1** could also coordinate with the Zn (II) ion. Additionally, the N atom of **1** appears to have a slight coordination with the Zn (II) ion. Our MD result indicates that the coordination distance between the N atom and the Zn (II) ion is greater than 3 Å (3.4 Å), the coordination bond is thus not marked in Figure 2B. These results suggest that the Zn (II) ion is important for the binding of **1**. Previously, Pombeiro et al.<sup>49, 50</sup> reported the crystal structure of compound **1** analogs and Cu (II)/Ni (II) ion. Our model binding mode of compound **1** with a Zn (II) ion is similar to those of the crystal structures of compound **1** analogs and Cu (II)/Ni (II) ion. Similar to Figure 2A, the hydrogen bonds between Asp289 and the NH moiety of **1** are retained. Compared with Figure 2A, the hydrogen bond between the nitro group of **1** and the OH moiety of Ser268 is retained, but the Thr290 is far from the nitro group of **1**. Indeed, the active site of FBA-II is highly conserved. According to the crystal structure of Ec-FBA-II,<sup>31</sup> the phosphate group of Ec-FBA-II could form a hydrogen bonds with Ser267, Lys325, Thr289 and Gly227. In our present model, the nitro group of **1** is located in the phosphate subsite of Ca-FBA-II. The nitro could form one hydrogen bond with Ser268, which corresponds to Ser267 in Ec-FBA-II. Therefore, the nitro group could perhaps play the role of a phosphate group in certain cases. After the MD simulation, one of the carbonyl groups of compound **1** was rotated approximately 180 degrees compared with those groups optimized by XO (Figure 2A). This result indicates that one of the carbonyl groups of **1** is rotatable and cannot easily form a

stable hydrogen-bond with surrounding residues. Using the complex conformation of Ca-FBA-II and **1** optimized by MD (Figure 2B), the corresponding binding free energy was calculated by XO methods to be -6.3 kcal/mol (corresponding to  $K_d = 24 \mu\text{M}$ ). This theoretical result is in the same order of magnitude as the experimental  $\text{IC}_{50}$  value ( $17 \mu\text{M}$ ).

**Rational design, optimization and synthesis of hit compounds.** To obtain more active hit compounds against Ca-FBA-II, a structure optimization and design route of compound **1** was next performed in terms of the binding mode of **1** to Ca-FBA-II that was described above, as illustrated in Figure 4. Starting from compound **1**, the simple substituent groups, such as **1a – s**, were first evaluated, and the results are summarized in Table 1. The position of the nitro group on the benzene ring has a substantial impact on the Ca-FBA-II activity. Compound **1** with the nitro substituent at the  $\text{R}^2$  position of the benzene ring exhibits high Ca-FBA-II inhibition (96 %), while compound **1a** with a nitro group at the  $\text{R}^3$  position exhibits no inhibitory activity against Ca-FBA-II (14 %). Therefore, the nitro group in the  $\text{R}^2$  position is favorable for the inhibition of Ca-FBA-II. According to the binding-mode of **1** to Ca-FBA-II (Figure 2B), the compound with the nitro group in the  $\text{R}^2$  position is favorable to forming a hydrogen bond with the surrounding residues (Ser268) in Ca-FBA-II. As  $\text{R}^2$  and  $\text{R}^3$  were fixed to hydrogen, the variants of  $\text{R}^1$  position (**1b–f**) show that the compound (**1f**) with hydroxyl group in  $\text{R}^1$  position exhibit higher Ca-FBA-II inhibitory activity ( $\text{IC}_{50} = 38 \mu\text{M}$ ) than the other variants. This result further confirms that, in accordance with the binding modes in Figure 2B, the coordination between the hydroxyl group and the Zn (II) ion is important to the binding of the hit compounds. As  $\text{R}^1$  and  $\text{R}^3$  were fixed to hydrogen, variants of  $\text{R}^2$  (**1g–n**) were subsequently explored. The compound (**1n**) with a nitro group in the  $\text{R}^2$  position exhibited higher inhibitory activity against Ca-FBA-II ( $\text{IC}_{50} = 20 \mu\text{M}$ ) than the others  $\text{R}^2$  variants. This finding further confirms that the nitro group in the  $\text{R}^3$  position

could form a hydrogen bond with Ser268, and the nitro group could possibly play the role of a phosphate group in certain cases. However, according to the binding mode of compound **1** in Figure 2B, the hydroxyl group and sulfonic acid group, which are similar to the nitro group, could indeed form hydrogen bonds with Ser268. Nevertheless, the solvation effect of a hydroxyl group and sulfonic acid group should be larger than that of a nitro group. For this reason, the energies of solvation of **1l**, **1m** and **1n** were next calculated at the wb97xd/6-31G\*-smd theory level using the Gaussian 09 software package, which are of 17.9 kcal/mol, 23.5 kcal/mol and 14.5 kcal/mol, respectively. The larger solvation effect counteracts the binding of the compound to Ca-FBA-II. Thus, compound **1n** exhibits a higher inhibitory activity against Ca-FBA-II than **1l** or **1m**. Regarding the structure-activity relationship (SAR) analysis mentioned above, the hydroxyl group in the R<sup>1</sup> position and the nitro group in the R<sup>3</sup> position are favorable for Ca-FBA-II inhibition by the hit compounds.

Regarding the binding mode in Figure 2B, one of the methyl groups of **1** is surrounded by the OH moiety of Thr38 and the NH<sub>2</sub> moieties of Gln293 and Arg332. Therefore, we hypothesized that, when the methyl in **1** is replaced by the amino group in **1s**, a hydrogen bond between the amino and surrounding residues could be formed, which might result in an increase in the corresponding inhibitory activities of the hit compounds. However, as listed in Table 1, the inhibitory activity of compound **1s** (IC<sub>50</sub> = 20 μM) is close to that of compound **1** (IC<sub>50</sub> = 17 μM).

Taken together, one can observe that it is hard to remarkably increase the Ca-FBA-II inhibitory activities of the hit compounds by varying the substituents groups of compound **1**. Additionally, some compound **1** analogues likely exist in tautomeric form in solvents.<sup>49</sup> Therefore, it was necessary for us to modify the framework of **1**. As illustrated in Figure 2B, one of the acetyl groups in compound **1** is located at the entrance of the active site of Ca-FBA-II, and no

1  
2  
3 remarkable hydrogen bond between this acetyl group and the surrounding residues can be  
4  
5 observed. Therefore, we next questioned whether developing compounds with only one acetyl  
6  
7 group would affect the Ca-FBA-II activity. Compounds **2** and **2a** were thus synthesized and  
8  
9 evaluated. Due to the synthesis difficulty, the hydroxyl group could not be introduced into the  
10  
11 benzene ring of compounds **2** and **2a**. As listed in Table 2, compound **2** exhibited no inhibitory  
12  
13 activity against Ca-FBA-II. To analyze the reason why **2** could not inhibit Ca-FBA-II, **2** was  
14  
15 docked into Ca-FBA-II by Surflex-Dock, and the probable binding-mode of **2** shown in  
16  
17 illustrated in Figure 5A, in which the Arg332 in the active site of Ca-FBA-II is nearby one of the  
18  
19 acetyl group of compound **1**. Thus, we supposed that if the methyl group in **2** were replaced by  
20  
21 the benzene group in **2a**, a  $\pi$ - $\pi$  interaction between the benzene ring of **2a** and Arg332 in Ca-  
22  
23 FBA-II could be formed. The possible binding mode of **2a** and Ca-FBA-II was also analyzed by  
24  
25 Surflex-Dock software, as illustrated in Figure 5B. As expected, compound **2a** exhibits a higher  
26  
27 inhibitory activity against Ca-FBA-II ( $IC_{50}=26\ \mu M$ ) than **2**, as listed in Table 2.  
28  
29  
30  
31  
32  
33

34 It should be noticed from Figure 5B that the only coordination interactions are between the  
35  
36 hydrazine group of **2a** and Zn (II), with a coordination distance of 2.8 Å, which is remarkably  
37  
38 shorter than that of **1** (Figure 2B). This finding suggests that the coordination between the  
39  
40 hydrazine group and Zn (II) plays a major role in influencing the Ca-FBA-II inhibition of the hit  
41  
42 compounds. To increase the interaction between the hydrazine of the hit compound and Zn (II),  
43  
44 we attempted to design and synthesize phenylhydrazone derivatives, such as **3** and **3a-l**, as listed  
45  
46 in Table 3, together with their corresponding inhibitions rates of enzymatic. For those  
47  
48 compounds with high inhibition rates (> 70%),  $IC_{50}$  values were also determined, and antifungal  
49  
50 assays were conducted. The enzymatic assay results demonstrate that the Ca-FBA-II inhibitory  
51  
52 activities of most of these compounds are higher, with  $IC_{50}$  value of 2.7–20  $\mu M$ . In particular,  
53  
54  
55  
56  
57  
58  
59  
60

compound **3g** exhibited the highest inhibition against Ca-FBA-II ( $IC_{50} = 2.7 \mu M$ ). The possible binding modes of the representative compound **3g** and Ca-FBA-II were also analyzed using the DOX strategy, as illustrated in Figure 6.

As shown in Figure 6, on the left of compound **3g**, the nitro group could form hydrogen bonds with the surrounding Ser268 and Thr290 residues in Ca-FBA-II, which is similar to the binding modes of compounds **1**, **2** and **2a**. As we designed above, the coordination distance ( $2.2 \text{ \AA}$ ) between the hydrazone group of **3g** and Zn (II) is shorter than that ( $2.8 \text{ \AA}$ ) of **2a**. As previously documented<sup>51</sup>, the hydrazone group easily forms a coordination bond with metals, therefore, compounds with hydrazone groups usually exhibit high biological activity. This is most likely the major reason why most of the phenylhydrazone derivatives (**3**, **3a–l**) possess highly inhibitory activity against Ca-FBA-II. On the right side of **3g**, the  $\pi$ – $\pi$  interaction between the benzene group and Arg332 can be observed. In addition, hydrogen bonds between the nitro group and Arg332 can also be found. Furthermore, the nitro group of benzene on the right side of compound **3g** ( $R^1$  position in Table 3) was replaced by other substituents to evaluate the corresponding Ca-FBA-II inhibitory activities. As seen in Table 3, when the 4' position of benzene was substituted by  $CH_3$ ,  $CF_3$  or H, the corresponding compounds exhibited weak inhibitory activities against Ca-FBA-II, as in **3**, **3a** and **3b**. However, the introduction of benzene, halogen, CN or  $NO_2$  at the 4' position of benzene led to a high inhibition of Ca-FBA-II by the hit compounds, such as **3c–g**, with  $IC_{50}$  values of  $2.7 - 12.6 \mu M$ . In particular, compound **3k** also showed a high level of Ca-FBA-II inhibition ( $IC_{50} = 6.0 \mu M$ ). Therefore, one could conclude that the compounds with conjugated and hydrogen-bond acceptor group at the  $R^1$  position of phenylhydrazone derivatives, such as **3c–g** and **3k**, have potentially higher Ca-FBA-II inhibitory activities than the other compounds. This suggests that for phenylhydrazone derivatives, the  $\pi$ – $\pi$

interaction between the conjugate group and the Arg332 is very important for their Ca-FBA-II inhibitory activities. Notably, compound **3g** not only could form  $\pi$ - $\pi$  interaction between nitrobenzene and Arg332, but also could form a hydrogen bond between a nitro group and Arg332, resulting in the highest inhibitory activity against Ca-FBA-II for compound **3g**.

To examine the interaction of **3g** and Ca-FBA-II, we have mutated the R332, T290 and S62 to Ala (Table 4), respectively. As listed in Table 4, R332A and T290A substitutions result in the 60-fold (101  $\mu$ M) and 130-fold (230.4  $\mu$ M) increase of  $K_i$  values compared with wild Ca-FBA-II (1.7  $\mu$ M). These experimental results indicate that R332 and T290 are significantly important to the binding of compound **3g** and Ca-FBA-II. In comparison, the  $K_i$  value of S62A (31.5  $\mu$ M) exhibit ~15-fold increase than that of wild Ca-FBA-II. This suggest that the interaction between S62 and compound **3g** is exist. However, the effect of R332 and T290 on the inhibitory activity of compound **3g** is smaller than S62, the possible explain is that the hydrogen-bond distances of compound **3g** and R332 and T290 is 2.2 Å, which is shorter than that (2.5 Å) of compound **3g** and S62, as can be noticed From Figure 6. These experiment are consistent with our theoretical results. Furthermore, we also mutated the residue D289, which is far from the active site of Ca-FBA-II and hasn't remarkable interactions with compound **3g**, to Ala. As expect, compound **3g** exhibit similar D289A inhibitory activities (3.1  $\mu$ M) to wild Ca-FBA-II (1.7 3.1  $\mu$ M). Thus, we further believe that our mutant results are reliable.

To examine the effect of the substituent group in the R<sup>2</sup> position of the third type of hit compounds on Ca-FBA-II inhibition, compounds **3i** and **3j** were also synthesized. As listed in Table 3, the Ca-FBA-II inhibitory rate of compound **3i** (61 %) is similar to that of **3** (43 %), indicating that the methyl group in the R<sup>2</sup> position slightly affects the Ca-FBA-II activity.



In a comparison, most of the phenylhydrazone derivatives (**3**, **3a–m**) exhibit greater Ca-FBA-II inhibition than the other hit compounds (**1**, **1a–s**, **2**, **2a**). As analyzed above, we inferred that the key reason is the increase in the coordination interaction between the hydrazone group in phenylhydrazone derivatives and the Zn (II) ions in Ca-FBA-II. To further confirm this speculation, we selected compounds **3f** and **3g** as probe molecules and attempted to design and synthesize benzoylhydrazone derivatives, such as **4** and **4a**, as listed in Table 5. We anticipated that the introduction of a carbonyl group near the hydrazine group, such as in **4** or **4a**, might be unfavorable for the coordination of the hydrazone group and the Zn (II) ions in Ca-FBA-II. As expected, compounds **4** (21 %) and **4a** (59 %) exhibited poor inhibitory activities against Ca-FBA-II compared with compounds **3f** (100 %) and **3g** (100 %). These results confirm to some extent that the hydrazone group is very important to the Ca-FBA-II inhibitory activities of the hit compounds.

**Antifungal evaluation.** To examine the antifungal activities of the hit compounds, those phenylhydrazone derivatives with high Ca-FBA-II inhibitions rates (**3c–h**, **3j–l**) were further assayed using a standard procedure for the inhibition of the growth of cultivated *C. albicans* (SC5314), *C. glabrata* (537) and *C. tropicalis*. The MIC<sub>80</sub> value of the control drug (fluconazole (FCZ)) was 0.5 µg/mL, which is in accordance with previous values.<sup>52</sup> Our results showed that none of our tested compounds exhibited a remarkable inhibitory activity (MIC<sub>80</sub> > 64 µg/mL) against *C. albicans* and *C. tropicalis*. Compound **3f** exhibited potential inhibitions (MIC<sub>80</sub> = 4 µg/mL) of *C. glabrata* (537). Compounds **3g** (MIC<sub>80</sub> = 16 µg/mL) and **3l** (MIC<sub>80</sub> = 64 µg/mL) displayed moderate inhibition of *C. glabrata* (537). The dose response curves of compounds **3f** and **3g** in the inhibition of the growth of cultivated *C. glabrata* (537) are illustrated in Figure S5. To our knowledge, several FBA-II inhibitors have been reported previously,<sup>16, 18, 26, 27</sup> however,

1  
2  
3 none of these inhibitors have demonstrated inhibitory activities against microorganisms to date.  
4  
5 This is the first report of FBA-II inhibitors with *in vitro* antifungal activities. The discrepancy  
6  
7 between the inhibitions of Ca-FBA-II and the antifungal assays can be partly explained by the  
8  
9 fact that the present hit compounds cannot easily cross biological membranes.  
10  
11

12  
13 As is known, the currently available azole antifungal agents can disrupt the cell membrane,  
14  
15 therefore, we hypothesized that the combination of azole drugs and our hit compounds may  
16  
17 facilitate the crossing of biological membranes by the hit compounds, which in turn could  
18  
19 enhance their antifungal activities. Especially, due to the extensive use of azoles drugs in humans,  
20  
21 the resistance of pathogenic microorganisms to current drug is a significant threat to public  
22  
23 health.<sup>12, 13</sup> Therefore, combined with FCZ (8  $\mu\text{g/mL}$ ), the potencies of our synthesized  
24  
25 phenylhydrazone analogues against the resistant *Candida* strains (100 and 103), which are  
26  
27 resistant to known azoles drugs ( $\text{MIC}_{80} > 1024 \mu\text{g/mL}$ ), were tested. As listed in Table 6, the  
28  
29  $\text{MIC}_{80}$  values of our synthesized phenylhydrazone analogues alone against are greater than 64  
30  
31  $\mu\text{g/mL}$ , and the  $\text{MIC}_{80}$  of FCZ alone is greater than 1024  $\mu\text{g/mL}$ . However, compounds **3d**, **3f**,  
32  
33 **3g**, **3k** and **3l** in combination with FCZ (8  $\mu\text{g/mL}$ ) resulted in remarkably greater inhibition than  
34  
35 that of either compound alone. Synergistic interactions were observed for these five hit  
36  
37 compounds. The combination index (CI) is regard as the gold standard for defining the  
38  
39 synergism of drug-drug interactions.<sup>53-55</sup> CI values=1 represent an additive effect; CI values < 1  
40  
41 and > 1 indicate synergistic and antagonistic interactions, respectively. Our calculated CI value  
42  
43 (Table 5) of compounds **3c–g**, **3k** and **3l**, in combination with the FCZ, were well below 0.02, at  
44  
45 0.004 to 0.02, pointing toward a pronounced synergistic activity<sup>10</sup>. Over all, the combination  
46  
47 therapy experiments have provided us the first proof that our novel Ca-FBA-II inhibitors, such as  
48  
49 **3d**, **3f**, **3g**, **3k** and **3l**, can combine with the known azole drugs to treat resistant fungi infections,  
50  
51  
52  
53  
54  
55  
56  
57  
58  
59  
60

which are resistant to known azole drugs. These compounds are worth developing as new antifungal therapies.

## CONCLUSIONS

FBA-II has always been regarded as a potent and particularly attractive new target for the discovery of drugs to combat invasive bacterial and fungal infections because of its occurrence in pathogenic microbes (bacteria, alga and fungi) and its absence in animals. Several inhibitors of FBA-II have been reported, but none of these inhibitors have antifungal effects. By jointly using a specific protocols of docking-based virtual screening, accurate binding-conformation evaluation strategy, a series of novel inhibitors of Ca-FBA-II were rationally designed, optimized and synthesized, and their inhibitory activities were examined by enzymatic and antifungal assay. Following a further study of SAR analysis, the inhibitors (**3c**, **3e–g**, **3j**) and **3k** with the high inhibitory activity against Ca-FBA-II ( $IC_{50} < 10 \mu M$ ) were designed. In particular, the compound **3g** was the most potent ( $IC_{50} = 2.7 \mu M$ ). Furthermore, compounds **1** and **3g** were selected as representative molecules for further analysis, and the probable binding modes between these two hit compounds and the active site of Ca-FBA-II were proposed by using a combination of the DOX strategy, MD simulations and enzymatic assays. The SAR analysis of the designed compounds can be consistently explained according to our proposed binding-modes of **1** and **3g** to Ca-FBA-II. These results revealed that the hydrazine group is a favorable scaffold for Ca-FBA-II inhibitors. It should be noticed that the compounds **3f**, **3g** and **3l** possessed not only high Ca-FBA-II inhibitory activities, but also moderate antifungal activities against *C. glabrata* ( $MIC_{80} = 4\text{--}64 \mu g/mL$ ). Moreover, compounds **3g**, **3l** and **3k** in combination with FCZ ( $8 \mu g/mL$ ) displayed significantly synergistic antifungal activities ( $MIC_{80} < 0.0625 \mu g/mL$ ) against resistant *Candida* strains, that are resistant to known azoles drugs ( $MIC_{80} > 1024 \mu g/mL$ ). To our

knowledge, this is the first report of FBA-II inhibitors with antifungal activities against wild type and resistant strains of *Candida*. This positive result confirmed that it is practical to use FBA-II as a potential target for the discovery of drugs fighting against the invasive bacterial and fungal infections. The present enzymatic and antifungal assay results suggest that the rational design of Ca-FBA-II inhibitors adopted in this study will be a promising road to the discovery of novel drugs against azole-resistant fungal pathogens of humans in the future.

## EXPERIMENTAL SECTIONS

**Sequence alignment and homology modeling.** The amino acid sequence of FBA-II from *C. albicans* (accession number in NCBI: 224471817) was aligned with that of Ec-FBA (PDB ID: 1B57)<sup>31</sup> using the program ClustalW2. Based on the sequence alignment, the structure of Ca-FBA-II was built by using the SWISSMODEL server<sup>32</sup>, employing the crystallographic structure of 1B57 (GI: 6980738) as the protein template. A dimeric structure of Ca-FBA-II was constructed via the combination of the two subunit. The Zn (II) ion were copy from the template structure. The dimeric conformation of Ca-FBA-II were then optimized by SYBYL-X1.3 with AMBER force field.<sup>56, 57</sup>

**Molecular dynamics (MD) simulations of Ca-FBA-II complex with compound 1.** To confirm the binding mode of probe molecule 1, MD simulations were performed by using the PMEMD module of AMBER 12 package,<sup>47</sup> based on the optimized Ca-FBA-II complex with compound 1. The partial atomic charges of compound 1 were calculated by restricted electrostatic potential (RESP)<sup>58</sup> fitting, which is implemented in the Antechamber module. The interactions between Zn (II) ion and protein was treated strictly by van der waals and coulomb forces.<sup>59</sup> The protein parameters were used by AMBER ff10 force field, whereas the general AMBER force field (GAFF) for the parameters of compound 1. The Na (I) ions were used to

neutralize the system, and then an octahedral box of TIP3P water molecules, which extended 10 Å from any given atom of Ca-FBA-II, were selected for solvation.<sup>60</sup> The MD was simulated with constant pressure and temperature (1 bar at 300 K) at periodic boundary conditions. The temperature was maintained at 300 K using the weak-coupling algorithm. The SHAKE algorithm<sup>61</sup> was used to constrain the bonds with hydrogen atoms. the long-range electrostatic interactions were calculated by Particle Mesh Ewald.<sup>62</sup> The non-bond cutoff was set as 10 Å. Equilibration was also monitored by combining the stability of the temperature, energies and densities of the system, as well as the RMSD values of the backbone atoms.

**XO calculations.** The relative stability of multiple possible protein-inhibitor binding-modes were obtained by XO calculation. XO method is a hybrid theoretical chemistry tool based on ONIOM and divide&conquer method designed to provide accurate quantum chemical description for large systems, which has been documented in previous publications.<sup>63, 64</sup> Our present computation system included the inhibitor molecule and the drug binding pocket involving the residues within 10 Å from any atom of the inhibitors. The inhibitor and surrounding residues were treated with  $\omega$ B97xD/6-311++G\*\*//6-31G\* level of theory while the rest of the system was considered using PM6 theory. The high level region was divided to 3 fragments for the XO calculation. In the free energy calculations, the solvation effect was considered employing SMD method. The entropy was obtained by frequency analysis of the inhibitor.

**PAINS Screening.** The hit compounds with high enzymatic inhibition against Ca-FBA-II ( $IC_{50} < 15 \mu M$ ) were screened by the Pan Assay Interference Compounds (PAINS) remover tool (Sybyl X1.3<sup>65</sup> and FAFDrug 3.0 server<sup>66</sup>) to remove the possible PAINS compounds. The results indicate that all of our active compounds in this study have passed the PAINS filter.

### General Synthetic methods.

The hit compounds **1a–s** in this study were prepared as previous documents,<sup>67</sup> which were from a diazonium solution and  $\beta$ -diketone, with sodium acetate in acetonitrile at a temperature below 5 °C (Scheme S1). The diazonium solution was prepared using a substituted aniline with  $\text{NaNO}_2$  and  $\text{HBF}_4$  in acetonitrile at a temperature below 5 °C. The  $\text{NaNO}_2$  was added in portions because the reaction was vigorous and highly exothermic. The hit compounds **2** and **2a** were prepared from a diazonium solution and ethyl acetoacetate with potassium acetate and 36%  $\text{HCl}$  in an aqueous potassium hydroxide solution at a temperature below 5 °C (Scheme S2), as documented previously.<sup>68</sup> The diazonium solution was prepared using a substituted aniline with  $\text{NaNO}_2$  and  $\text{HBF}_4$  in acetonitrile at a temperature below 5 °C. Compounds **3**, **3a–m** were prepared<sup>69</sup> by phenylhydrazine and benzaldehyde in absolute ethanol (Scheme S3). According to the previous report,<sup>70</sup> The hit compounds **4** and **4a** were prepared by benzoyl hydrazine and benzaldehyde in absolute ethanol, as illustrated in Scheme S4.

**Enzyme inhibition activities and Site-Directed Mutagenesis.** The half maximal inhibitory concentration ( $\text{IC}_{50}$ ) of some hit compounds with high inhibitions have been examined at the Ca-FBA-II recombinant protein level by linear regression analysis in Origin 7.5 program package to evaluate the inhibitory activities of these compounds. The gene sequence of Ca-FBA-II was obtained from NCBI (XM\_717597.1).<sup>71</sup> Ca-FBA-II was expressed in *E. coli* BL21(DE3) cells, it was purified as previous document.<sup>72</sup> Commercial preparations from Sigma of glycerol 3-phosphate dehydrogenase (GPDH) from rabbit muscle and triosephosphate isomerase (TIM) from rabbit muscle were used. The inhibitory activity of hit compounds against Ca-FBA-II were determined by using an NADH linked enzymatic assay.<sup>73, 74</sup> The activity of cleavage reaction was examined in Tris-potassium-acetate buffer (0.1 M, pH 7.4, with 0.2 M potassium-acetate for

FBA-II), NADH (0.6 mM), glycerol 3-phosphate dehydrogenase (GPDH, 0.3 U, Sigma), triosephosphate isomerase (TIM, 1 U, Sigma), aldolase (0.4  $\mu\text{g/mL}$ ), and various concentrations of FBP (50–1000  $\mu\text{M}$ ) in a cuvette to give the final volume of 0.4 mL. The reaction was carried out for 5 min at 30  $^{\circ}\text{C}$ . The decrease of NADH absorbance at 340 nm was monitored by spectrophotometer (SpectraMax M5, Molecular Devices). The kinetic data were analyzed by Nonlinear regression by using the Hill relation yields a maximal specific activity ( $V_{\text{max}}$ ) of 70 U/mg, a  $k_{\text{cat}}$  of 46  $\text{s}^{-1}$  and a  $K_{\text{m}}$  of 61  $\mu\text{M}$ , which is similar to the literature value ( $K_{\text{m}} = 85 \mu\text{M}$ ).<sup>16</sup>

To determine the  $\text{IC}_{50}$  values, the initial rate data taken from a saturating substrate concentration, a fixed effector concentration, and systematically varied concentrations of test compounds were fit to a Hill equation,  $V = V_0 - (V_0 - V_{\infty}) / ((I_{0.5} / I)^n + 1)^{75}$ , where  $V$ ,  $V_0$ , and  $V_{\infty}$  are the velocity, maximum velocity (at  $I = 0$ ), and the limiting velocity (at  $I$  saturating), respectively;  $n$  is the Hill coefficient associated with inhibitor. All kinetic parameters of Ca-FBA-II were determined by plotting the velocity vs substrate concentrations according to Hill equation in origin 7.0 software. The inhibition assay was run under a concentration of compounds **3c** and **3g**, as illustrated in Figure 7.

Mutations were performed by introducing specific base changes into a double-stranded DNA plasmid. All site-directed mutagenesis procedures were accomplished as our previous publication<sup>44</sup>. Additionally, the parental methylated and hemimethylated DNA were digested by Nde I and BamH I restriction enzyme (Fermentas, China). Expression and purification of mutant Ca-FBA-II were similar to those of wild-type enzyme. By using SDS-PAGE, the identical motilities were exhibited for all purified enzymes (wild and mutant) to ensure the purities more than 95%.

**Antifungal Assays.** Antifungal activities of some of the hit compounds, FCZ was measured by means of the minimum inhibitory concentration (MIC) of the *C. albicans* strain (SC5314), *C. glabrata* strain (537) and *C. tropicalis* in 96-well micro-test plates, as given in document M27-A3<sup>76</sup> and M38-A2<sup>77</sup> from the National Committee for Clinical Laboratory Standards (NCCLS). Additionally, the MIC<sub>80</sub> values were defined as being the minimum concentrations of the drugs that inhibited the growth by more than 80% in comparison with that of the drug-free wells. The *C. albicans* strain (SC5314), *C. glabrata* strain (537) and *C. tropicalis* were obtained from the Second Military Medical University. The test compounds were dissolved in DMSO, and serially diluted in the range of 0.125 to 64.0 µg/mL for the checker-board micro-dilution assay. DMSO was used as a growth control, FCZ was used as controls against the tested fungi. The microtiter plates were incubated at 35 °C for 48 h for the *Candida* species. The optical density was monitored at 630 nm and the background absorptions were subtracted from the value of each well.

Assays were performed on resistant *Candida* strains (100 and 103) in term of broth microdilution checkerboard method. The final combination concentrations ranged from 0.125 to 64 µg/mL or 0.016 to 8 µg/mL for test compounds and 8 µg/mL for FCZ. The final concentrations of test compounds are from 0.125 to 64 µg/mL, and FCZ is ranged from 2 to 1024 µg/mL. The combination index (CI) was calculated according to the following equation:

$$CI = \frac{MIC_{mA}}{MIC_{aA}} + \frac{MIC_{mB}}{MIC_{aB}},$$
 where MIC<sub>mA</sub> and MIC<sub>aA</sub> are the MICs of the combination and alone of test compounds, and MIC<sub>mB</sub> and MIC<sub>aB</sub> are the MICs of the combination and alone of FCZ, respectively.



**Supporting Information.** Supporting Information is Available: Experimental procedures, analytical data, enzyme assays, and biological evaluation.

## AUTHOR INFORMATION

### Corresponding Author

\*To whom correspondence should be addressed. Phone: +86-27-67862022. Fax: +86-27-67862022. E-mails: [renyl@mail.ccnu.edu.cn](mailto:renyl@mail.ccnu.edu.cn); [jianwan@mail.ccnu.edu.cn](mailto:jianwan@mail.ccnu.edu.cn)

### Author Contributions

The manuscript was written through contributions of all authors. All authors have given approval to the final version of the manuscript. ‡These authors contributed equally. (Match statement to author names with a symbol)

### Notes

The authors declare no competing financial interest.

## ACKNOWLEDGMENT

This work was supported by the Natural Science Foundation of China (Nos. 21572077, 21472061, 21373094, 21202056 and 21272089), the Program for the PCSIRT (No. IRT0953), and the self-determined research funds of CCNU from the colleges' basic research and operation of MOE (Nos. CCNU16A02041 and CCNU14A05006).

## ABBREVIATIONS

FBA-I, class I fructose-1,6-bisphosphate aldolase; FBA-II, class II fructose-1,6-bisphosphate aldolase; Ca-FBA-II, class II fructose-1,6-bisphosphate aldolase from *C. albicans*; Ec-FBA-II, class II fructose-1,6-bisphosphate aldolase from *E. coli*; class I fructose-1,6-bisphosphate

aldolase from rabbit muscle (Ra-FBA-I); DHAP, dihydroxyacetonephosphate; GAP, glyceraldehyde 3-phosphate; GPDH, glycerol 3-phosphate dehydrogenase; TIM, triosephosphate isomerase; FBP, fructose-1,6-biphosphate; MD, molecular dynamic; BCE, binding-conformation evaluation; ONIOM, our-own N-layered integrated molecular orbital and molecular mechanics; ONIOM3, three-layer ONIOM; Fluconazole (FCZ); DOX, Docking, ONIOM and XO

## REFERENCES

1. Fonvielle, M.; Coincon, M.; Daher, R.; Desbenoit, N.; Kosieradzka, K.; Barilone, N.; Gicquel, B.; Sygusch, J.; Jackson, M.; Therisod, M., Synthesis and biochemical evaluation of selective inhibitors of class II fructose bisphosphate aldolases: towards new synthetic antibiotics. *Chem. Eur. J.* **2008**, *14*, 8521-8529.
2. Calderone, R. A.; Fonzi, W. A., Virulence factors of *Candida albicans*. *Trends Microbiol.* **2001**, *9*, 327-335.
3. Calderone, R. A., *Candida and Candidiasis*. ASM Press, Washington, D. C. **2002**.
4. Odds, F. C., *Candida and Candidosis*, 2nd ed. Bailliere Tindall, London, United Kingdom. **1988**.
5. Vermes, A., Flucytosine: a review of its pharmacology, clinical indications, pharmacokinetics, toxicity and drug interactions. *J. Antimicrob. Chemother.* **2000**, *46*, 171-179.
6. Goldman, W. E.; Butts, A.; Krysan, D. J., Antifungal Drug Discovery: Something Old and Something New. *PLoS Pathog.* **2012**, *8*, e1002870-73.
7. Ashbee, H. R.; Barnes, R. A.; Johnson, E. M.; Richardson, M. D.; Gorton, R.; Hope, W. W., Therapeutic drug monitoring (TDM) of antifungal agents: guidelines from the British Society for Medical Mycology. *J. Antimicrob. Chemother.* **2013**, *69*, 1162-1176.
8. Odds, F. C.; Brown, A. J. P.; Gow, N. A. R., Antifungal agents: mechanisms of action. *Trends Microbiol.* **2003**, *11*, 272-279.
9. Cui, J. H.; Ren, B.; Tong, Y. J.; Dai, H. Q.; Zhang, L. X., Synergistic combinations of antifungals and anti-virulence agents to fight against *Candida albicans*. *Virulence* **2015**, *6*, 362-371.

10. Troskie, A. M.; Rautenbach, M.; Delattin, N.; Vosloo, J. A.; Dathe, M.; Cammue, B. P.; Thevissen, K., Synergistic activity of the tyrocidines, antimicrobial cyclodecapeptides from *Bacillus aneurinolyticus*, with amphotericin B and caspofungin against *Candida albicans* biofilms. *Antimicrob. Agents Ch.* **2014**, *58*, 3697-3707.
11. Baddley, J. W.; Pappas, P. G., Antifungal Combination Therapy. *Drugs* **2005**, *65*, 1461-1480.
12. Soulsby, E. J., Resistance to antimicrobials in humans and animals. *BMJ* **2005**, *331*, 1219-1220.
13. Edmond, M. B.; Wallace, S. E.; McClish, D. K.; Pfaller, M. A.; Jones, R. N.; Wenzel, R. P., Nosocomial bloodstream infections in United States hospitals: a three-year analysis. *Clin. Infect. Dis.* **1999**, *29*, 239-244.
14. Zhang, W.; Ramamoorthy, Y.; Kilicarslan, T.; Nolte, H.; Tyndale, R. F.; Sellers, E. M., Inhibition of cytochromes P450 by antifungal imidazole derivatives. *Drug Metab. Dispos.* **2002**, *30*, 314-318.
15. Gefflaut, T.; Blonski, C.; Perie, J.; Willson, M., Class I aldolases: substrate specificity, mechanism, inhibitors and structural aspects. *Prog. Biophys. Mol. Biol.* **1995**, *63*, 301-340.
16. Daher, R.; Coincon, M.; Fonvielle, M.; Gest, P. M.; Guerin, M. E.; Jackson, M.; Sygusch, J.; Therisod, M., Rational design, synthesis, and evaluation of new selective inhibitors of microbial class II (zinc dependent) fructose bis-phosphate aldolases. *J. Med. Chem.* **2010**, *53*, 7836-7842.
17. Haake, V.; Zrenner, R.; Sonnewald, U.; Stitt, M., A moderate decrease of plastid aldolase activity inhibits photosynthesis, alters the levels of sugars and starch, and inhibits growth of potato plants. *Plant J.* **1998**, *14*, 147-157.
18. Li, Z.; Liu, Z.; Cho, D. W.; Zou, J.; Gong, M.; Breece, R. M.; Galkin, A.; Li, L.; Zhao, H.; Maestas, G. D.; Tierney, D. L.; Herzberg, O.; Dunaway-Mariano, D.; Mariano, P. S., Rational design, synthesis and evaluation of first generation inhibitors of the *Giardia lamblia* fructose-1,6-biphosphate aldolase. *J. Inorg. Biochem.* **2011**, *105*, 509-517.
19. Pegan, S. D.; Rukserree, K.; Franzblau, S. G.; Mesecar, A. D., Structural Basis for Catalysis of a Tetrameric Class IIa Fructose 1,6-Bisphosphate Aldolase from *Mycobacterium tuberculosis*. *J. Mol. Biol.* **2009**, *386*, 1038-1053.
20. Wehmeier, U., Molecular cloning, nucleotide sequence and structural analysis of the

Streptomyces galbus DSM40480 fda gene: the S. galbus fructose-1,6-bisphosphate aldolase is a member of the class II aldolases. *FEMS Microbiol. Lett.* **2001**, *197*, 53-58.

21. Kobayashi, K.; Ehrlich, S. D.; Albertini, A.; Amati, G.; Andersen, K. K.; Arnaud, M.; Asai, K.; Ashikaga, S.; Aymerich, S.; Bessieres, P.; Boland, F.; Brignell, S. C.; Bron, S.; Bunai, K.; Chapuis, J.; Christiansen, L. C.; Danchin, A.; Debarbouille, M.; Dervyn, E.; Deuerling, E.; Devine, K.; Devine, S. K.; Dreesen, O.; Errington, J.; Fillinger, S.; Foster, S. J.; Fujita, Y.; Galizzi, A.; Gardan, R.; Eschevins, C.; Fukushima, T.; Haga, K.; Harwood, C. R.; Hecker, M.; Hosoya, D.; Hullo, M. F.; Kakeshita, H.; Karamata, D.; Kasahara, Y.; Kawamura, F.; Koga, K.; Koski, P.; Kuwana, R.; Imamura, D.; Ishimaru, M.; Ishikawa, S.; Ishio, I.; Le Coq, D.; Masson, A.; Mauel, C.; Meima, R.; Mellado, R. P.; Moir, A.; Moriya, S.; Nagakawa, E.; Nanamiya, H.; Nakai, S.; Nygaard, P.; Ogura, M.; Ohanan, T.; O'Reilly, M.; O'Rourke, M.; Pragai, Z.; Pooley, H. M.; Rapoport, G.; Rawlins, J. P.; Rivas, L. A.; Rivolta, C.; Sadaie, A.; Sadaie, Y.; Sarvas, M.; Sato, T.; Saxild, H. H.; Scanlan, E.; Schumann, W.; Seegers, J. F.; Sekiguchi, J.; Sekowska, A.; Seror, S. J.; Simon, M.; Stragier, P.; Studer, R.; Takamatsu, H.; Tanaka, T.; Takeuchi, M.; Thomaides, H. B.; Vagner, V.; van Dijl, J. M.; Watabe, K.; Wipat, A.; Yamamoto, H.; Yamamoto, M.; Yamamoto, Y.; Yamane, K.; Yata, K.; Yoshida, K.; Yoshikawa, H.; Zuber, U.; Ogasawara, N., Essential Bacillus subtilis genes. *Proc Natl Acad Sci U S A* **2003**, *100*, 4678-4683.

22. Jacobs, M. A.; Alwood, A.; Thaipisuttikul, I.; Spencer, D.; Haugen, E.; Ernst, S.; Will, O.; Kaul, R.; Raymond, C.; Levy, R.; Chun-Rong, L.; Guenther, D.; Bovee, D.; Olson, M. V.; Manoil, C., Comprehensive transposon mutant library of *Pseudomonas aeruginosa*. *Proc. Natl Acad. of Sci. USA* **2003**, *100*, 14339-14344.

23. Liberati, N. T.; Urbach, J. M.; Miyata, S.; Lee, D. G.; Drenkard, E.; Wu, G.; Villanueva, J.; Wei, T.; Ausubel, F. M., An ordered, nonredundant library of *Pseudomonas aeruginosa* strain PA14 transposon insertion mutants. *Proc Natl Acad Sci U S A* **2006**, *103*, 2833-2838.

24. Song, J. H.; Ko, K. S.; Lee, J. Y.; Baek, J. Y.; Oh, W. S.; Yoon, H. S.; Jeong, J. Y.; Chun, J., Identification of essential genes in *Streptococcus pneumoniae* by allelic replacement mutagenesis. *Mol. Cells* **2005**, *19*, 365-374.

25. Rodaki, A.; Young, T.; Brown, A. J., Effects of depleting the essential central metabolic enzyme fructose-1,6-bisphosphate aldolase on the growth and viability of *Candida albicans*: implications for antifungal drug target discovery. *Eukaryot. Cell* **2006**, *5*, 1371-1377.

26. Desvergnès, S.; Courtiol-Legourd, S.; Daher, R.; Dabrowski, M.; Salmon, L.; Therisod,

- M., Synthesis and evaluation of malonate-based inhibitors of phosphosugar-metabolizing enzymes: class II fructose-1,6-bis-phosphate aldolases, type I phosphomannose isomerase, and phosphoglucose isomerase. *Bioorg. Med. Chem.* **2012**, *20*, 1511-1520.
27. Daher, R.; Therisod, M., Highly Selective Inhibitors of Class II Microbial Fructose Bis-phosphate Aldolases. *ACS Med. Chem. Lett.* **2010**, *1*, 101-104.
28. Rao, L.; Chi, B.; Ren, Y.; Li, Y.; Xu, X.; Wan, J., DOX: A new computational protocol for accurate prediction of the protein–ligand binding structures. *J. Comput. Chem.* **2016**, *37*, 336-344.
29. Moser, D.; Wisniewska, J. M.; Hahn, S.; Achenbach, J.; Buscató, E. I.; Klingler, F.-M.; Hofmann, B.; Steinhilber, D.; Proschak, E., Dual-Target Virtual Screening by Pharmacophore Elucidation and Molecular Shape Filtering. *ACS Med. Chem. Lett.* **2012**, *3*, 155-158.
30. Larkin, M. A.; Blackshields, G.; Brown, N. P.; Chenna, R.; McGettigan, P. A.; McWilliam, H.; Valentin, F.; Wallace, I. M.; Wilm, A.; Lopez, R.; Thompson, J. D.; Gibson, T. J.; Higgins, D. G., Clustal W and Clustal X version 2.0. *Bioinformatics* **2007**, *23*, 2947-2948.
31. Hall, D. R.; Leonard, G. A.; Reed, C. D.; Watt, C. I.; Berry, A.; Hunter, W. N., The crystal structure of Escherichia coli class II fructose-1,6-bisphosphate aldolase in complex with phosphoglycolohydroxamate reveals details of mechanism and specificity. *J. Mol. Biol.* **1999**, *287*, 383-394.
32. Schwede, T.; Kopp, J.; Guex, N.; Peitsch, M. C., SWISS-MODEL: an automated protein homology-modeling server. *Nucleic Acids Res.* **2003**, *31*, 3381-3385.
33. *Sybyl X version 1.3*; Tripos Inc.: St. Louis, MO, 2011; <http://www.tripos.com> (accessed Nov 12, 2011).
34. Laskowski, R. A.; MacArthur, M. W.; Moss, D. S.; Thornton, J. M., PROCHECK: a program to check the stereochemical quality of protein structures. *J. Appl. Crystallogr.* **1993**, *26*, 283-291.
35. Cristobal, S.; Zemla, A.; Fischer, D.; Rychlewski, L.; Elofsson, A., A study of quality measures for protein threading models. *BMC Bioinformatics* **2001**, *2*, 5-19.
36. Wiederstein, M.; Sippl, M. J., ProSA-web: interactive web service for the recognition of errors in three-dimensional structures of proteins. *Nucleic. Acids Res.* **2007**, *35*, w407-w410.
37. Sippl, M. J., Recognition of errors in three-dimensional structures of proteins. *Proteins Struct. Funct. Bioinf.* **1993**, *17*, 355-362.

38. Benkert, P.; Schwede, T.; Tosatto, S., QMEANclust: estimation of protein model quality by combining a composite scoring function with structural density information. *BMC Struct. Biol.* **2009**, *9*, 35-51.
39. de la Paz Santangelo, M.; Gest, P. M.; Guerin, M. E.; Coincon, M.; Pham, H.; Ryan, G.; Puckett, S. E.; Spencer, J. S.; Gonzalez-Juarrero, M.; Daher, R.; Lenaerts, A. J.; Schnappinger, D.; Therisod, M.; Ehrt, S.; Sygusch, J.; Jackson, M., Glycolytic and non-glycolytic functions of *Mycobacterium tuberculosis* fructose-1,6-bisphosphate aldolase, an essential enzyme produced by replicating and non-replicating bacilli. *J. Biol. Chem.* **2011**, *286*, 40219-40231.
40. Lipinski, C. A.; Lombardo, F.; Dominy, B. W.; Feeney, P. J., Experimental and computational approaches to estimate solubility and permeability in drug discovery and development settings. *Adv. Drug Del. Rev.* **2012**, *64*, Supplement, 4-17.
41. Hindle, S.; Rarey, M.; Buning, C.; Lengauer, T., Flexible docking under pharmacophore type constraints. *J. Comput. Aided Mol. Des.* **2002**, *16*, 129-149.
42. Jain, A., Surflex-Dock 2.1: Robust performance from ligand energetic modeling, ring flexibility, and knowledge-based search. *J. Comput. Aided Mol. Des.* **2007**, *21*, 281-306.
43. Jain, A. N., Surflex: Fully Automatic Flexible Molecular Docking Using a Molecular Similarity-Based Search Engine. *J. Med. Chem.* **2003**, *46*, 499-511.
44. Li, D.; Gui, J.; Li, Y. J.; Feng, L. L.; Han, X. Y.; Sun, Y.; Sun, T. L.; Chen, Z. G.; Cao, Y.; Zhang, Y.; Zhou, L.; Hu, X. P.; Ren, Y. L.; Wan, J., Structure-Based Design and Screen of Novel Inhibitors for Class II 3-Hydroxy-3-methylglutaryl Coenzyme A Reductase from *Streptococcus Pneumoniae*. *J. Chem. Inf. Model.* **2012**, *52*, 1833-1841.
45. Zhang, Q. Y.; Li, D.; Wei, P.; Zhang, J.; Wan, J.; Ren, Y. L.; Chen, Z. G.; Liu, D. L.; Yu, Z. N.; Feng, L. L., Structure-Based Rational Screening of Novel Hit Compounds with Structural Diversity for Cytochrome P450 Sterol 14 alpha-Demethylase from *Penicillium digitatum*. *J. Chem. Inf. Model.* **2010**, *50*, 317-325.
46. Han, X.; Zhu, X.; Zhu, S.; Wei, L.; Hong, Z.; Guo, L.; Chen, H.; Chi, B.; Liu, Y.; Feng, L.; Ren, Y.; Wan, J., A Rational Design, Synthesis, Biological Evaluation and Structure-Activity Relationship Study of Novel Inhibitors against Cyanobacterial Fructose-1,6-bisphosphate Aldolase. *J. Chem. Inf. Model.* **2016**, *56*, 73-81.
47. Case, D. A.; Darden, T. A.; Cheatham, T. E.; Simmerling, C. L.; Wang, J.; Duke, R. E.; Luo, R.; Walker, R. C.; Zhang, W.; Merz, K. M.; Roberts, B.; Hayik, S.; Roitberg, A.; Seabra, G.;

Swails, J.; Götz, A. W.; Kolossváry, I.; Wong, K. F.; Paesani, F.; Vanicek, J.; Wolf, R. M.; Liu, J.; Wu, X.; Brozell, S. R.; Steinbrecher, T.; Gohlke, H.; Cai, Q.; Ye, X.; Wang, J.; Hsieh, M. J.; Cui, G.; Roe, D. R.; Mathews, D. H.; Seetin, M. G.; Salomon-Ferrer, R.; Sagui, C.; Babin, V.; Luchko, T.; Gusarov, S.; Kovalenko, A.; Kollman, P. A., University of California, San Francisco, 2012. AMBER 12.

48. Rao, L.; Zhang, I. Y.; Guo, W.; Feng, L.; Meggers, E.; Xu, X., Nonfitting protein-ligand interaction scoring function based on first-principles theoretical chemistry methods: development and application on kinase inhibitors. *J. Comput. Chem.* **2013**, *34*, 1636-1646.

49. Kopylovich, M. N.; Mahmudov, K. T.; Guedes da Silva, M. F. C.; Kirillov, A. M.; Pombeiro, A. J. L., Unusual shift of a nitro group in a phenylhydrazo- $\beta$ -diketone. *Dalton T.* **2011**, *40*, 12472-12478.

50. Mahmudov, K. T.; Kopylovich, M. N.; Silva, M. F. C. G. d.; Figiel, P. J.; Karabach, Y. Y.; Pombeiro, A. J. L., New copper(II) dimer with 3-(2-hydroxy-4-nitrophenylhydrazo)pentane-2,4-dione and its catalytic activity in cyclohexane and benzyl alcohol oxidations. *J. Mol. Catal. A: Chem.* **2010**, *318*, 44-50.

51. Pal, M. K.; Kushwah, N.; Wadawale, A. P.; Dey, S.; Sudarsan, V.; Jain, V. K., Monoorgano-gallium and -indium complexes derived from dianionic tridentate ONO Schiff bases: Synthesis, crystal structures and photoluminescence. *J. Organomet. Chem.* **2016**, *808*, 128-133.

52. Sheng, C.; Zhang, W.; Ji, H.; Zhang, M.; Song, Y.; Xu, H.; Zhu, J.; Miao, Z.; Jiang, Q.; Yao, J.; Zhou, Y.; Zhu, J.; Lü, J., Structure-Based Optimization of Azole Antifungal Agents by CoMFA, CoMSIA, and Molecular Docking. *J. Med. Chem.* **2006**, *49*, 2512-2525.

53. Chou, T. C., Drug Combination Studies and Their Synergy Quantification Using the Chou-Talalay Method. *Cancer Res.* **2010**, *70*, 440-446.

54. Chou, T. C.; Talalay, P., Quantitative analysis of dose-effect relationships: the combined effects of multiple drugs or enzyme inhibitors. *Adv. Enzyme Regul.* **1984**, *22*, 27-55.

55. Chou, T. C., Theoretical basis, experimental design, and computerized simulation of synergism and antagonism in drug combination studies. *Pharmacol. Rev.* **1970**, *326*, 261-270.

56. Cornell, W. D.; Cieplak, P.; Bayly, C. I.; Gould, I. R.; Merz, K. M.; Ferguson, D. M.; Spellmeyer, D. C.; Fox, T.; Caldwell, J. W.; Kollman, P. A., A Second Generation Force Field for the Simulation of Proteins, Nucleic Acids, and Organic Molecules. *J. Am. Chem. Soc.* **1995**, *117*,

5179-5197.

57. Wang, D.; Zhu, X.; Cui, C.; Dong, M.; Jiang, H.; Li, Z.; Liu, Z.; Zhu, W.; Wang, J.-G., Discovery of Novel Acetohydroxyacid Synthase Inhibitors as Active Agents against *Mycobacterium tuberculosis* by Virtual Screening and Bioassay. *J. Chem. Inf. Model.* **2013**, *53*, 343-353.

58. Wang, J. M.; Wang, W.; Kollman, P. A., Antechamber: An accessory software package for molecular mechanical calculations. *Abs. Pap. ACS* **2001**, 222, U403-U403.

59. Stote, R. H.; Karplus, M., Zinc binding in proteins and solution: a simple but accurate nonbonded representation. *Proteins* **1995**, *23*, 12-31.

60. Jorgensen, W. L.; Chandrasekhar, J.; Madura, J. D.; Impey, R. W.; Klein, M. L., Comparison of simple potential functions for simulating liquid water. *J. Chem. Phys.* **1983**, *79*, 926-935.

61. Krautler, V.; Van Gunsteren, W. F.; Hunenberger, P. H., A fast SHAKE: Algorithm to solve distance constraint equations for small molecules in molecular dynamics simulations. *J. Comput. Chem.* **2001**, *22*, 501-508.

62. Nam, K.; Gao, J. L.; York, D. M., An efficient linear-scaling Ewald method for long-range electrostatic interactions in combined QM/MM calculations. *J. Chem. Theory Comput.* **2005**, *1*, 2-13.

63. Guo, W.; Wu, A.; Zhang, I. Y.; Xu, X., XO: An extended ONIOM method for accurate and efficient modeling of large systems. *J. Comput. Chem.* **2012**, *33*, 2142-2160.

64. Rao, L.; Zhang, I. Y.; Guo, W.; Feng, L.; Meggers, E.; Xu, X., Nonfitting protein-ligand interaction scoring function based on first-principles theoretical chemistry methods: Development and application on kinase inhibitors. *J. Comput. Chem.* **2013**, *34*, 1636-1646.

65. Baell, J. B.; Holloway, G. A., New Substructure Filters for Removal of Pan Assay Interference Compounds (PAINS) from Screening Libraries and for Their Exclusion in Bioassays. *J. Med. Chem.* **2010**, *53*, 2719-2740.

66. Lagorce, D.; Sperandio, O.; Baell, J. B.; Miteva, M. A.; Villoutreix, B. O., FAF-Drugs3: a web server for compound property calculation and chemical library design. *Nucleic Acids Res.* **2015**, *43*, 200-207.

67. Kopylovich, M. N.; Mahmudov, K. T.; Guedes da Silva, M. F. C.; Figiel, P. J.; Karabach, Y. Y.; Kuznetsov, M. L.; Luzyanin, K. V.; Pombeiro, A. J. L., Ortho-Hydroxyphenylhydrazo- $\beta$ -



Diketones: Tautomery, Coordination Ability, and Catalytic Activity of Their Copper(II) Complexes toward Oxidation of Cyclohexane and Benzylic Alcohols. *Inorg. Chem.* **2011**, *50*, 918-931.

68. Al-Saleh, B.; Hilmy, N. M.; El-Asasery, M. A.; Elnagdi, M. H., Microwaves in Organic Synthesis: Synthesis of Pyridazinones, Phthalazinones and Pyridopyridazinones from 2-Oxo-arylhydrazones under Microwave Irradiation. *J. Heterocycl. Chem.* **2007**, *38*, 1575-1581.

69. Backes, G. L.; Neumann, D. M.; Jursic, B. S., Synthesis and antifungal activity of substituted salicylaldehyde hydrazones, hydrazides and sulfohydrazides. *Bioorg. Med. Chem.* **2014**, *22*, 4629-36.

70. You, Z. L.; Xian, D. M.; Zhang, M.; Cheng, X. S.; Li, X. F., Synthesis, biological evaluation, and molecular docking studies of 2,5-substituted-1,4-benzoquinone as novel urease inhibitors. *Bioorg. Med. Chem.* **2012**, *20*, 4889-4894.

71. Jones, T.; Federspiel, N. A.; Chibana, H.; Dungan, J.; Kalman, S.; Magee, B. B.; Newport, G.; Thorstenson, Y. R.; Agabian, N.; Magee, P. T.; Davis, R. W.; Scherer, S., The diploid genome sequence of *Candida albicans*. *Proc Natl Acad Sci U S A* **2004**, *101*, 7329-7334.

72. Li, F. Q.; Ma, C. F.; Shi, L. N.; Lu, J. F.; Wang, Y.; Huang, M.; Kong, Q. Q., Diagnostic value of immunoglobulin G antibodies against *Candida enolase* and fructose-bisphosphate aldolase for candidemia. *BMC Infect. Dis.* **2013**, *13*, 253-261.

73. Racker, E., Spectrophotometric measurement of hexokinase and phosphohexokinase activity. *J. Biol. Chem.* **1947**, *167*, 843-854.

74. Blonski, C.; De Moissac, D.; Perie, J.; Sygusch, J., Inhibition of rabbit muscle aldolase by phosphorylated aromatic compounds. *Biochem. J* **1997**, *323*, 71-77.

75. Wilkins, J. C.; Homer, K. A.; Beighton, D., Analysis of *Streptococcus mutans* Proteins Modulated by Culture under Acidic Conditions. *Appl. Environ. Microbiol.* **2002**, *68*, 2382-2390.

76. Clinical and Laboratory Standards Institute/National Committee for Clinical Laboratory Standards: Reference method for broth dilution antifungal susceptibility testing of Yeast. Approved Standard, edn 3; Document M27-A3. Wayne, PA: Clinical and Laboratory Standards Institute. **2009**.

77. Clinical and Laboratory Standards Institute/National Committee for Clinical Laboratory Standards: Reference method for broth dilution antifungal susceptibility testing of Yeast. Approved Standard, edn 3; Document M38-A2. Wayne, PA: Clinical and Laboratory Standards

Institute. 2008.

### Figure Captions

**Figure 1.** Mechanisms of class I and class II FBP aldolases

**Figure 2.** The proposed binding-mode of compound **1** into the active site of Ca-FBA-II optimized by XO (A) and MD simulations (B). The ribbons represent the helix and sheet of protein, the light blue stick represents the compound **1**, and the surrounding important residues were represented by the creamy white stick. The green dashed line represents the important interactions of the ligand and target enzyme.

**Figure 3.** Plots of the molecular dynamic (MD) simulation time vs root-mean-square deviation (RMSD, in Å) of the all atoms of the Ca-FBA-II in complex with compound **1**. The black line

represents the rmsd of the entire enzyme and compound **1**, the pink line represents the corresponding rmsd of the compounds **1**.

**Figure 4.** The structure optimization routes of Ca-FBA-II inhibitors

**Figure 5.** The proposed binding modes of compounds **2** (A) and **2a** (B) into the active site of Ca-FBA-II docked by Surflex-Dock software. The ribbons represent the helix and sheet of protein, the light blue stick represents the compound, and the surrounding important residues were represented by the creamy white stick. The green dashed line represents the important interactions of the ligand and target enzyme.

**Figure 6.** The proposed binding-mode of compound **3g** into the active site of Ca-FBA-II optimized by XO. The ribbons represent the helix and sheet of protein, the light blue stick represents the compound **3g**, and the surrounding important residues were represented by the creamy white stick. The green dashed line represents the important interactions of the ligand and target enzyme.

**Figure 7.** The inhibition assay was run in the concentration range (0 – 50  $\mu$ M) of hit compounds **3c** and **3g**. The inhibition of DMSO was taken as blank control, for all hit compounds dissolved in DMSO.

1  
2  
3  
4  
5  
6  
7  
8  
9  
10  
11  
12  
13  
14  
15  
16  
17  
18  
19  
20  
21  
22  
23  
24  
25  
26  
27  
28  
29  
30  
31  
32  
33  
34  
35  
36  
37  
38  
39  
40  
41  
42  
43  
44  
45  
46  
47  
48  
49  
50  
51  
52  
53  
54  
55  
56  
57  
58  
59  
60

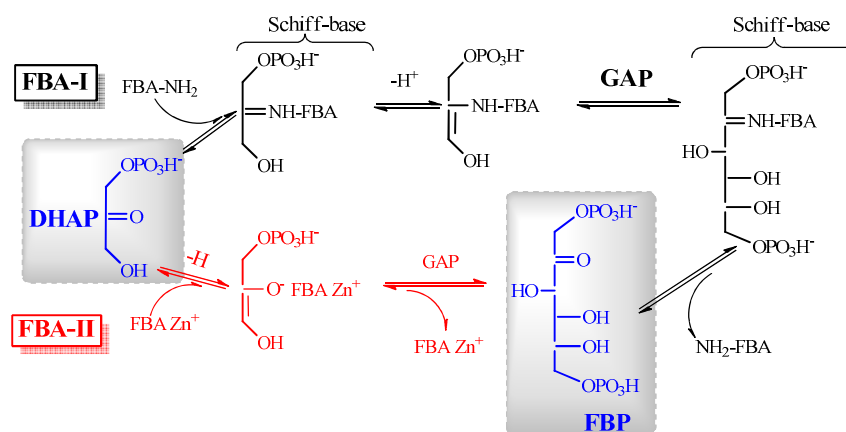


**Figure 1.** Mechanisms of class I and class II FBP aldolases

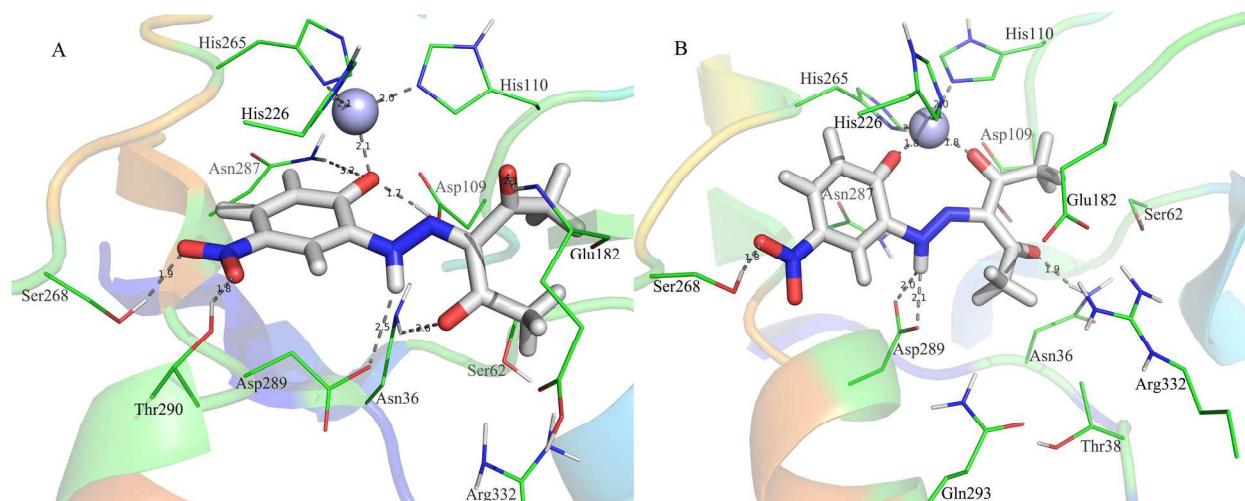


**Figure 2.** The proposed binding-mode of compound **1** into the active site of Ca-FBA-II optimized by XO (A) and MD simulations (B). The ribbons represent the helix and sheet of protein, the light blue stick represents the compound **1**, and the surrounding important residues were represented by the creamy white stick. The green dashed line represents the important interactions of the ligand and target enzyme.

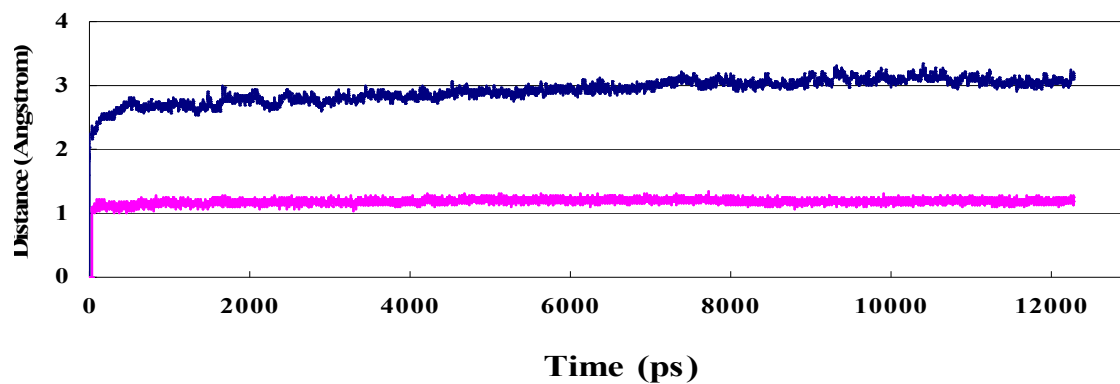


**Figure 3.** Plots of the molecular dynamic (MD) simulation time vs root-mean-square deviation (RMSD, in Å) of the all atoms of the Ca-FBA-II in complex with compound **1**. The black line represents the rmsd of the entire enzyme and compound **1**, the pink line represents the corresponding rmsd of the compounds **1**.

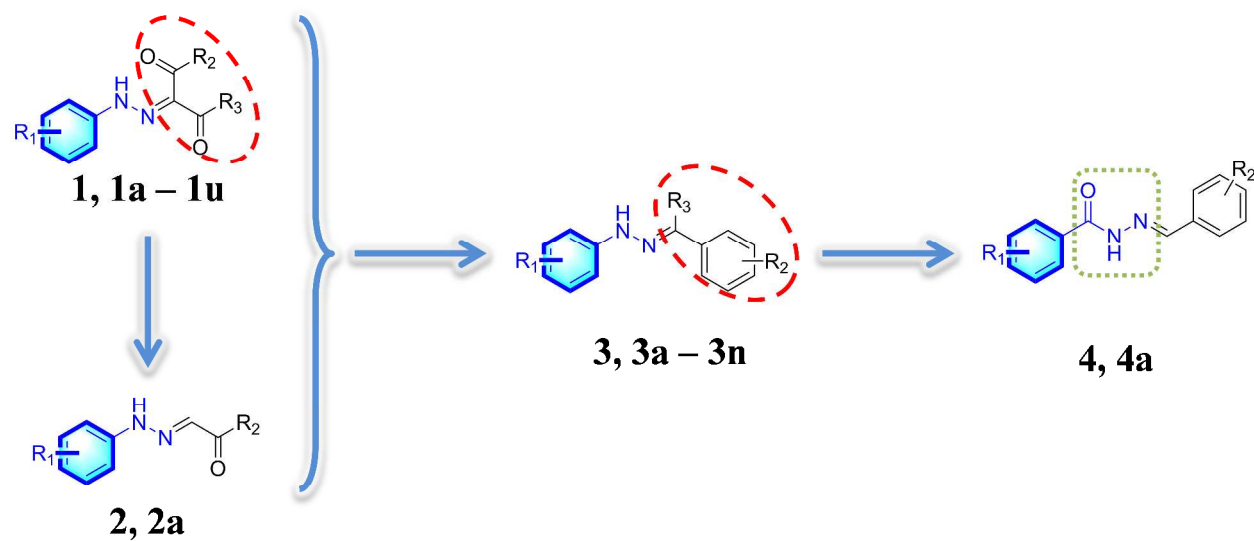
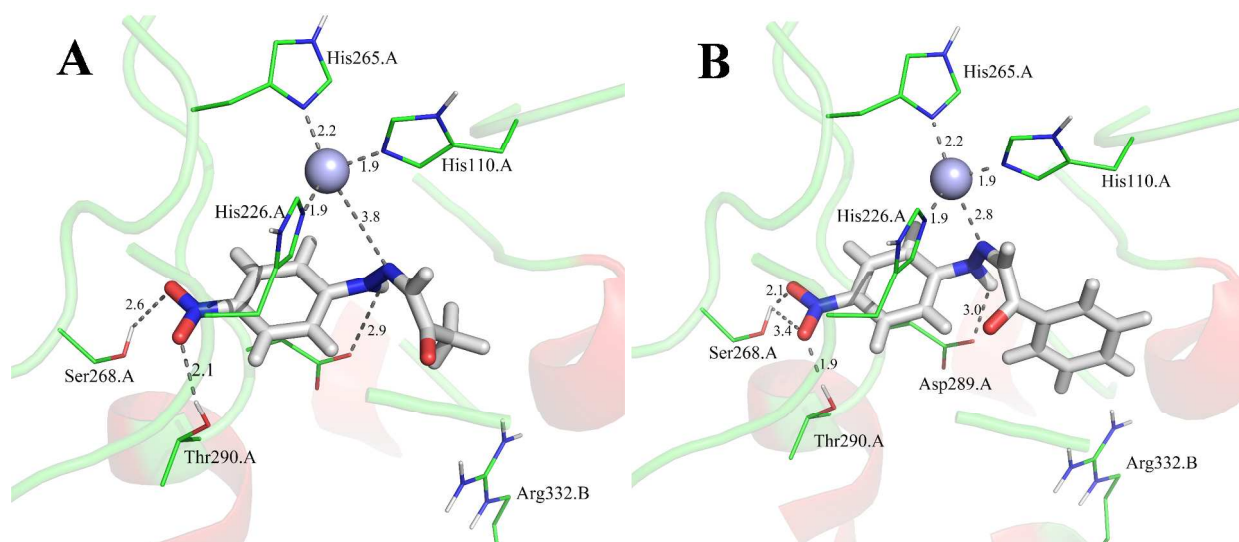
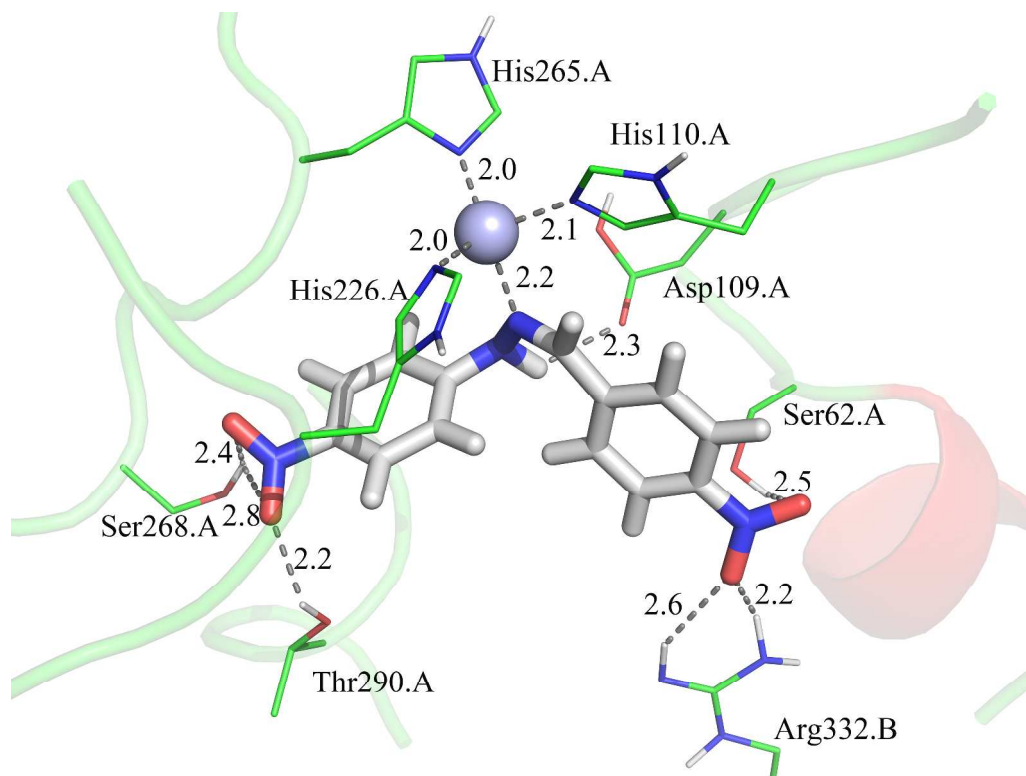


Figure 4. The structure optimization routes of Ca-FBA-II inhibitors





**Figure 5.** The proposed binding modes of compounds **2** (A) and **2a** (B) into the active site of Ca-FBA-II docked by Surflex-Dock software. The ribbons represent the helix and sheet of protein, the light blue stick represents the compound, and the surrounding important residues were represented by the creamy white stick. The green dashed line represents the important interactions of the ligand and target enzyme.



**Figure 6.** The proposed binding-mode of compound **3g** into the active site of Ca-FBA-II optimized by XO. The ribbons represent the helix and sheet of protein, the light blue stick represents the compound **3g**, and the surrounding important residues were represented by the creamy white stick. The green dashed line represents the important interactions of the ligand and target enzyme.

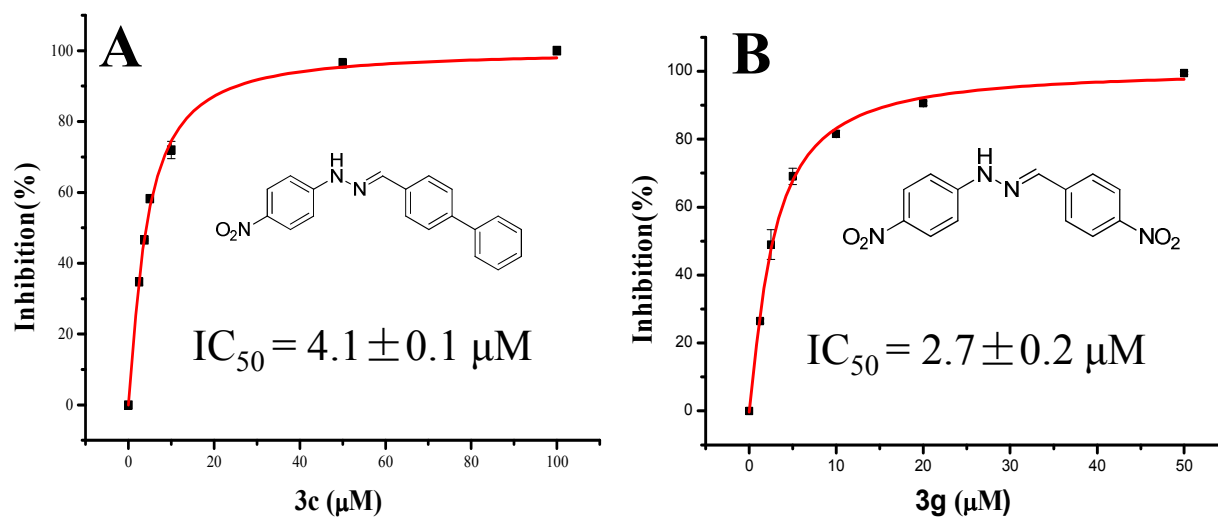


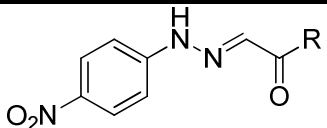
**Figure 7.** The inhibition assay was run in the concentration range (0 – 50  $\mu M$ ) of hit compounds **3c** (A) and **3g** (B). The inhibition of DMSO was taken as blank control for all hit compounds dissolved in DMSO.

**Table 1.** The inhibitory activities of the hit compounds (**1**, **1a – s**) against Ca-FBA-II

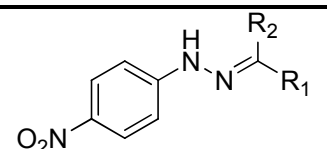
Compds	R <sup>1</sup>	R <sup>2</sup>	R <sup>3</sup>	R <sup>4</sup>	R <sup>5</sup>	Inhibitions <sup>a</sup>	IC <sub>50</sub> ( $\mu M$ )

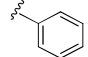
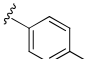
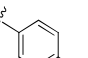
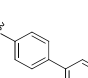
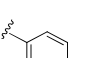
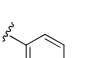
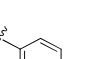
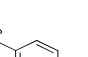
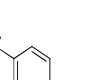
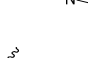
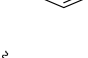
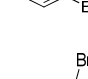
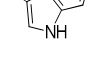
<b>1</b>	OH	NO <sub>2</sub>	H	CH <sub>3</sub>	CH <sub>3</sub>	96%	17±2
<b>1a</b>	OH	H	NO <sub>2</sub>	CH <sub>3</sub>	CH <sub>3</sub>	14%	/
<b>1b</b>	H	H	H	CH <sub>3</sub>	CH <sub>3</sub>	10%	/
<b>1c</b>	F	H	H	CH <sub>3</sub>	CH <sub>3</sub>	3%	/
<b>1d</b>	CH <sub>3</sub>	H	H	CH <sub>3</sub>	CH <sub>3</sub>	9%	/
<b>1e</b>	CN	H	H	CH <sub>3</sub>	CH <sub>3</sub>	16%	/
<b>1f</b>	OH	H	H	CH <sub>3</sub>	CH <sub>3</sub>	73%	38±1
<b>1g</b>	H	F	H	CH <sub>3</sub>	CH <sub>3</sub>	7%	/
<b>1h</b>	H	Cl	H	CH <sub>3</sub>	CH <sub>3</sub>	20%	/
<b>1i</b>	H	Br	H	CH <sub>3</sub>	CH <sub>3</sub>	27%	/
<b>1j</b>	H	Tz*	H	CH <sub>3</sub>	CH <sub>3</sub>	-8%	/
<b>1k</b>	H	TzCH <sub>2</sub>	H	CH <sub>3</sub>	CH <sub>3</sub>	5%	/
<b>1l</b>	H	OH	H	CH <sub>3</sub>	CH <sub>3</sub>	5%	/
<b>1m</b>	H	SO <sub>3</sub> H	H	CH <sub>3</sub>	CH <sub>3</sub>	14%	/
<b>1n</b>	H	NO <sub>2</sub>	H	CH <sub>3</sub>	CH <sub>3</sub>	92%	20±1
<b>1o</b>	CH <sub>3</sub>	NO <sub>2</sub>	H	CH <sub>3</sub>	CH <sub>3</sub>	65%	43±4
<b>1p</b>	COOH	NO <sub>2</sub>	H	CH <sub>3</sub>	CH <sub>3</sub>	10%	/
<b>1q</b>	NO <sub>2</sub>	NO <sub>2</sub>	H	CH <sub>3</sub>	CH <sub>3</sub>	1%	/
<b>1r</b>	Cl	NO <sub>2</sub>	H	CH <sub>3</sub>	CH <sub>3</sub>	68%	/
<b>1s</b>	OH	NO <sub>2</sub>	H	CH <sub>3</sub>	NH <sub>2</sub>	94%	20±2

<sup>a</sup> Percentage inhibition at 50 μM concentration

**Table 2.** The inhibitory activities of the hit compounds (**2**, **2a**) against Ca-FBA-II


Compds	R	Inhibition <sup>a</sup>	IC <sub>50</sub> (μM)
<b>2</b>	CH <sub>3</sub>	6%	/
<b>2a</b>	C <sub>6</sub> H <sub>5</sub>	91%	26±2

<sup>a</sup> Percentage inhibition at 50 μM concentration**Table 3.** The inhibitory activities of the hit compounds (**3**, **3a–I**) against Ca-FBA-II, together with the corresponding inhibition against *C. albicans* and antifungal assays


Compds	R <sub>1</sub>	R <sub>2</sub>	Inhibition <sup>a</sup>	IC <sub>50</sub> (μM)
<b>3</b>		H	43 %	/
<b>3a</b>		H	80 %	20 ± 1
<b>3b</b>		H	60 %	/
<b>3c</b>		H	92 %	4.1 ± 0.1
<b>3d</b>		H	94 %	12.6 ± 0.8
<b>3e</b>		H	91 %	6.4 ± 0.3
<b>3f</b>		H	100 %	9.4 ± 0.5
<b>3g</b>		H	100 %	2.7 ± 0.2
<b>3h</b>		H	83 %	25 ± 1
<b>3i</b>		CH <sub>3</sub>	62 %	/
<b>3j</b>		CH <sub>3</sub>	99 %	7.5 ± 0.3
<b>3k</b>		H	97 %	6.0 ± 0.3
<b>3l</b>		H	97 %	20 ± 1

<sup>a</sup> Percentage inhibition at 50 μM concentration

**Table 4.** The inhibitory constant ( $K_i$ ) of compounds **3g** against the wild and variants of Ca-FBA-

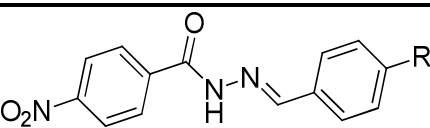
II

---

Wild	R332A	T290A	S62A	D289A
------	-------	-------	------	-------

$K_i$ ( $\mu\text{M}$ )	1.7	101.0	230.4	31.5	3.1
-------------------------	-----	-------	-------	------	-----

**Table 5.** The inhibitory activities of the hit compounds (**4**, **4a**) against Ca-FBA-II



Compds	R	Inhibition <sup>a</sup>
<b>4</b>	CN	21 %
<b>4a</b>	NO <sub>2</sub>	59 %

<sup>a</sup> Percentage inhibition at 50  $\mu\text{M}$  concentration

**Table 6.** The antifungal assays (MIC<sub>80</sub>  $\mu\text{g/mL}$ ) of the phenylhydrazone derivatives

Compds	<i>C. glabrata</i> (537)	Resistant strains (100/103) <sup>b</sup>	Synergistic Inhibitions+FCZ <sup>a</sup>			
			Resistant	CI	Resistant	CI



	strains 100 <sup>b</sup>				strain 103 <sup>b</sup>	
<b>3c</b>	>64	>64	2	0.020	1	0.016
<b>3d</b>	>64	>64	0.125	0.005	0.0625	0.004
<b>3e</b>	>64	>64	1	0.012	0.5	0.008
<b>3f</b>	4	>64	1	0.012	0.5	0.008
<b>3g</b>	16	>64	0.25	0.006	0.0625	0.004
<b>3h</b>	>64	>64	>64	>1	4	0.035
<b>3j</b>	/	>64	/	/	/	
<b>3k</b>	>64	>64	0.0625	0.004	0.0156	0.004
<b>3l</b>	64	>64	0.0625	0.004	0.03125	0.004
<b>FCZ</b>	0.5	>1024	>1024	/	>1024	/

<sup>a</sup>The MIC<sub>80</sub> values were tested combined with FCZ at 8 µg/mL; <sup>b</sup>The strains 100 and 103 from *Candida* are resistant to known azoles drugs.

Insert Table of Contents Graphic and Synopsis Here

